Towards a Virtual Geostationary Ocean Colour Satellite Using Ocean Colour Constellation Data

[1,2]Marco Bracaglia, [1]Gianluca Volpe, [1]Simone Colella, [1]Rosalia Santoleri, [3]Federica Braga, [1]Vittorio Ernesto Brando.

[1] Istituto di Scienze Marine (CNR-ISMAR), Via Fosso del Cavaliere 100, 00133, Roma, Italy
[2]Università degli Studi di Napoli Parthenope, Via Amm. F. Acton 38, 80133, Naples, Italy
[3]Istituto di Scienze Marine (CNR-ISMAR), Arsenale-Tesa 104, Castello 2737/F, 30122 Venice, Italy

Objective and study area

- **In coastal areas the optical properties of the water components have a large variability** on both spatial and temporal scale.
- Use of a single Ocean Colour (OC) polar sensor not sufficient to capture this variability, as it provides ~1 image a day of a basin at the middle latitudes.
- **OC geostationary sensors** provide multiple daily observations.
- Absent over the European Seas.
- **Objective:** Compensate the lack of an OC geostationary sensor over coastal environments, like the North Adriatic Sea (NAS), to have high temporal resolution observations of the optical properties.

Map of the NAS with the rivers of the basin.

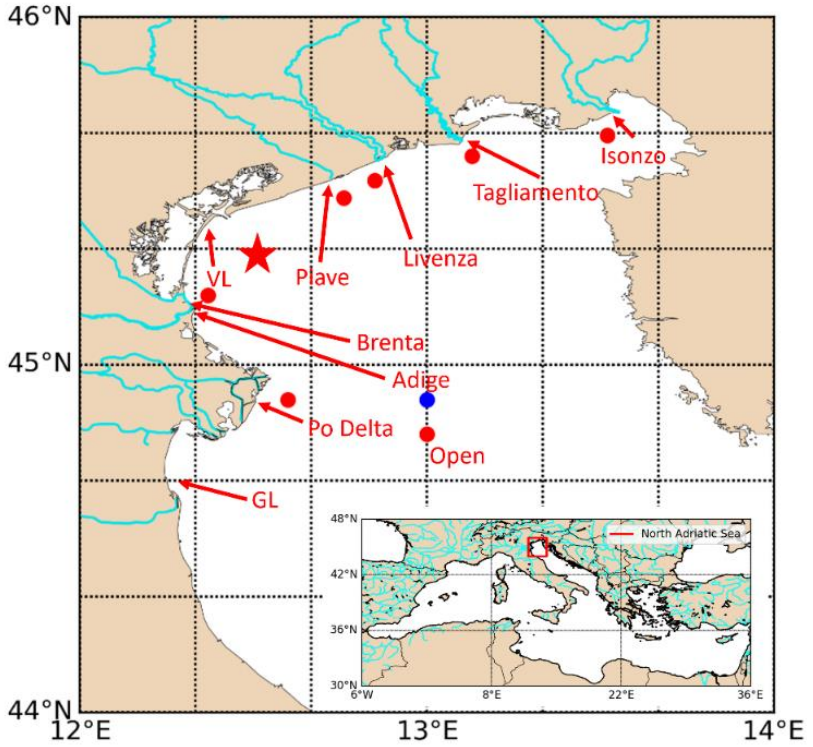

Babin et al., 2003a; Babin et al., 2003b; Blondeau-Patissier et al.,2009 ; Brando et al., 2012; Mouw et al., 2015; Ryu et al.,2012; Solidoro et al., 2009.

The Virtual Geostationary Ocean Colour Sensor (VGOCS) dataset

- Analysis ready dataset that contains NAS observations from several OCR polar sensors (2002-2019).
- Multiple images during the same day, to approach the temporal resolution of a geostationary satellite.
- **Inter-sensor differences**:
  - Different spatial and spectral resolution.
  - Different processing.
  - Different calibration accuracy.
  - Different viewing geometry.
- Differences between different images are due to bio-optical processes or **artefacts**?
- To **reduce the inter-sensor differences: satellite R_{rs} adjustment** based on the Acqua Alta Oceanographic Tower (AAOT) in situ data.

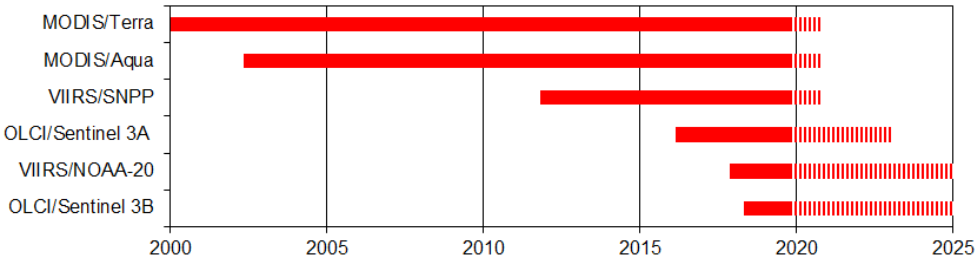

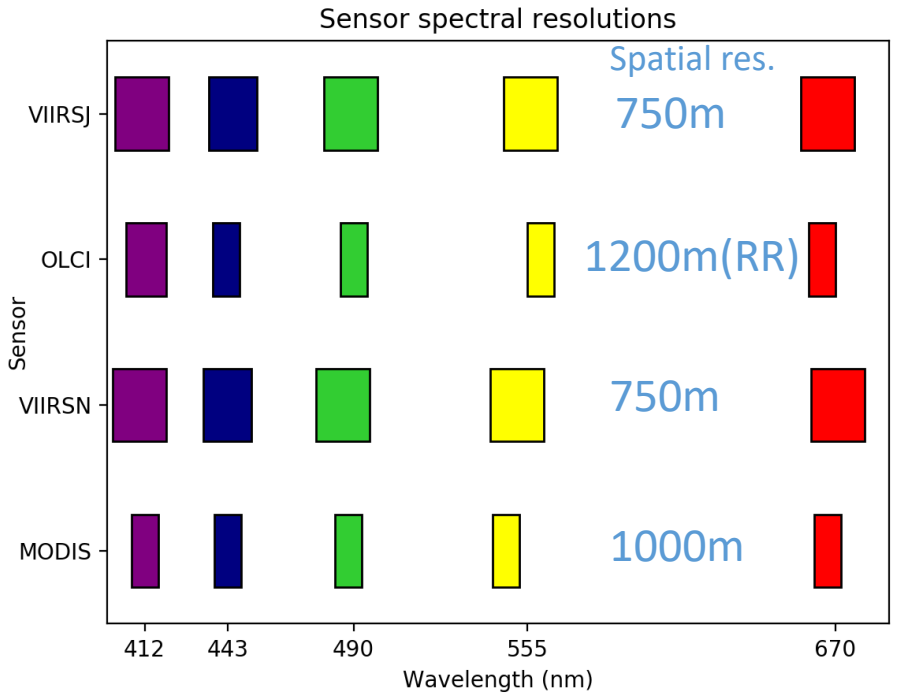

AQUA(A): MODIS-AQUA, TERRA(T): MODIS-TERRA,VIIRSN(V): VIIRS SUOMI-NPP, VIIRSJ(J): VIIRS NOAA-20, OLCI(O): OLCI S3A

Barnes & Hu, 2016 ; Cao et al., 2013; D'Alimonte et al. 2008; Donlon et al., 2012; Masuoka et al., 1998; Qi et al.,2017; Zibordi et al., 2006; Zibordi et al.,2009.

The VGOCS dataset

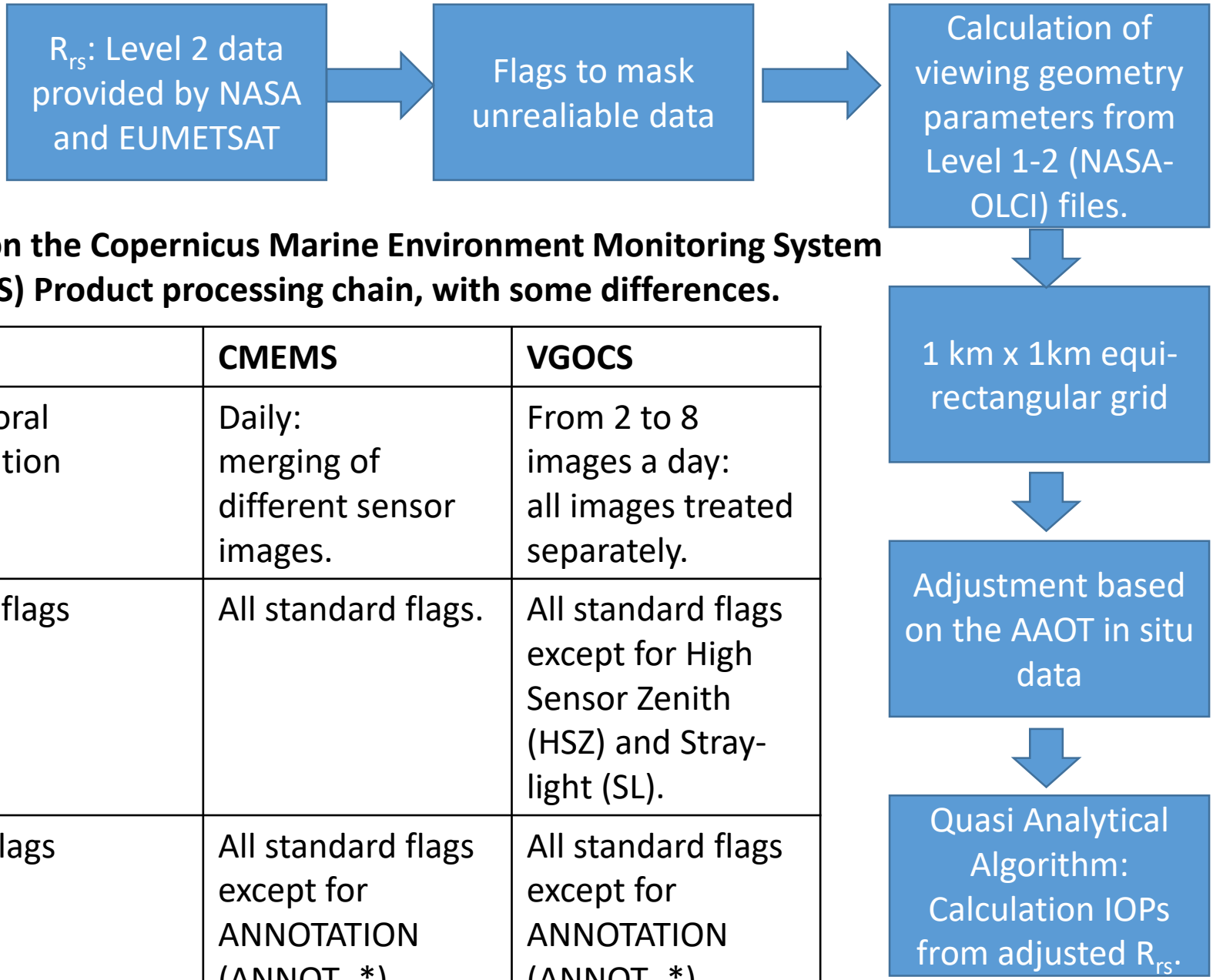

Based on the Copernicus Marine Environment Monitoring System (CMEMS) Product processing chain, with some differences.

	CMEMS	**VGOCS**
Temporal resolution	Daily: merging of different sensor images.	From 2 to 8 images a day: all images treated separately.
NASA flags	All standard flags.	All standard flags except for High Sensor Zenith (HSZ) and Stray-light (SL).
OLCI flags	All standard flags except for ANNOTATION (ANNOT_*).	All standard flags except for ANNOTATION (ANNOT_*).

Bracaglia et al., 2019 ; Lee et al., 2002; Volpe et al., 2019

The VGOCS dataset

Filename format: VGOCS_yyyyjjjhhmmss_X.nc
yyyy: year, jjj: julian day of the year ,hh: hour, mm: minute, ss: second, X: sensor label

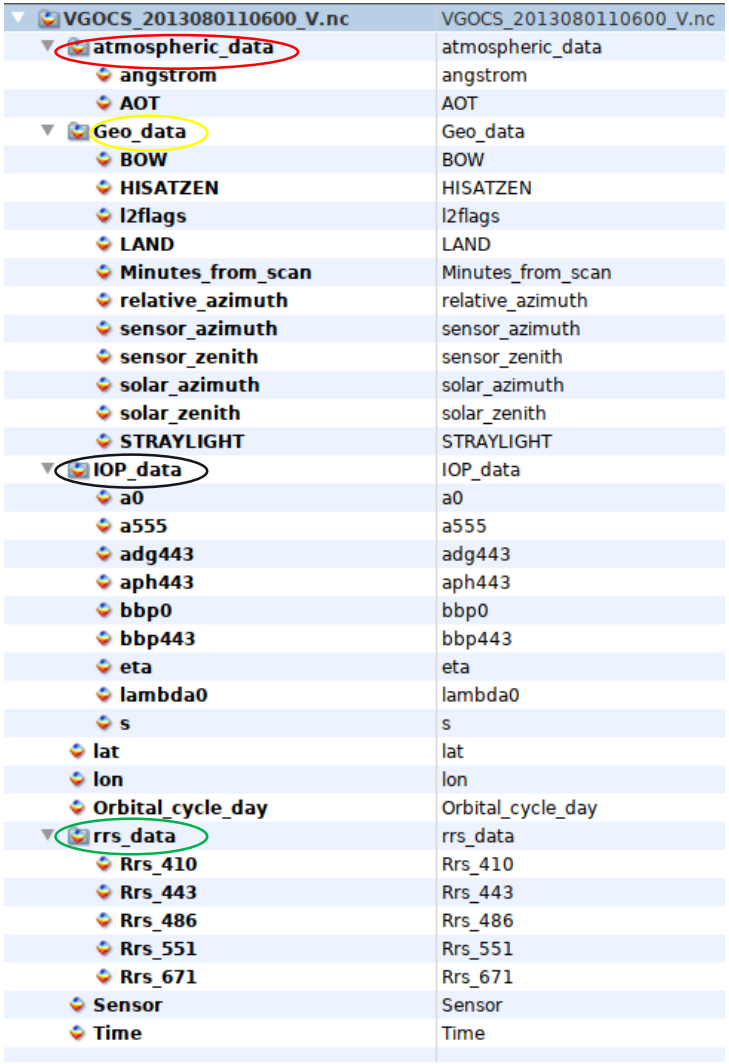

VGOCS_2013080110600_V.nc	VGOCS_2013080110600_V.nc
atmospheric_data	atmospheric_data
angstrom	angstrom
AOT	AOT
Geo_data	Geo_data
BOW	BOW
HISATZEN	HISATZEN
l2flags	l2flags
LAND	LAND
Minutes_from_scan	Minutes_from_scan
relative_azimuth	relative_azimuth
sensor_azimuth	sensor_azimuth
sensor_zenith	sensor_zenith
solar_azimuth	solar_azimuth
solar_zenith	solar_zenith
STRAYLIGHT	STRAYLIGHT
IOP_data	IOP_data
a0	a0
a555	a555
adg443	adg443
aph443	aph443
bbp0	bbp0
bbp443	bbp443
eta	eta
lambda0	lambda0
s	s
lat	lat
lon	lon
Orbital_cycle_day	Orbital_cycle_day
rrs_data	rrs_data
Rrs_410	Rrs_410
Rrs_443	Rrs_443
Rrs_486	Rrs_486
Rrs_551	Rrs_551
Rrs_671	Rrs_671
Sensor	Sensor
Time	Time

atmospheric_data:
Aerosol optical thickness at 86X nm and angstrom coefficient.

Geo_data:
Information about the flags, viewing geometry and time of the pixel observations.

IOP_data:
All the IOPs estimated from the QAA.

rrs_data:
All the R_{rs} bands used in the QAA at the native λ.

Multi-linear regression (MLR) adjustment

Different adjustment coefficients for different sensors.
TRAINING DATASET: coefficient calculation.
VALIDATION DATASET: match-up analyses.

$$\Delta R_{rs}(\lambda) = R_{rs}^{is}(\lambda) - R_{rs}^{or}(\lambda)$$

Estimation of the coefficients

$$< \Delta R_{rs}(\lambda) > = a_0^{sat} + \sum_{i=1}^{5} a_i^{sat} R_{rs}^{or}(\lambda_i) + a_6^{sat}\theta_v + a_7^{sat}\theta_s + a_8^{sat}\varphi$$

$$R_{rs}^{adj}(\lambda) = R_{rs}^{or}(\lambda) + < \Delta R_{rs}(\lambda) >$$

R_{rs}^{or}=original satellite R_{rs}
R_{rs}^{ad}=adjusted satellite R_{rs}
R_{rs}^{is}=in situ R_{rs}

θ_v= sensor zenith angle.
θ_s= solar zenith angle.
ϕ= relative azimuth angle.

Bracaglia et al., 2019; D'Alimonte et al., 2008; Melin et al. 2011; Zibordi et al., 2006; Zibordi et al.,2009

R_{rs} in situ data acquired at the Acqua Alta Oceanographic Tower (AAOT), part of the Aeronet-OC network and representative of most of the optical variability of the basin.

Giuseppe Zibordi from the Joint Research Center of the European Commission is acknowledged for establishing and maintaining the AAOT AERONET-OC site.

Multi-linear regression (MLR) adjustment

Different adjustment coefficients for different sensors.
TRAINING DATASET: coefficient calculation.
VALIDATION DATASET: match-up analyses.

$$\Delta R_{rs}(\lambda) = R_{rs}^{is}(\lambda) - R_{rs}^{or}(\lambda)$$

Estimation of the coefficients

$$< \Delta R_{rs}(\lambda) > = a_0^{sat} + \sum_{i=1}^{5} a_i^{sat} R_{rs}^{or}(\lambda_i) + a_6^{sat}\theta_v + a_7^{sat}\theta_s + a_8^{sat}\varphi$$

$$R_{rs}^{adj}(\lambda) = R_{rs}^{or}(\lambda) + < \Delta R_{rs}(\lambda) >$$

R_{rs}^{or}=original satellite R_{rs}
R_{rs}^{ad}=adjusted satellite R_{rs}
R_{rs}^{is}=in situ R_{rs}

θ_v= sensor zenith angle.
θ_s= solar zenith angle.
ϕ= relative azimuth angle.

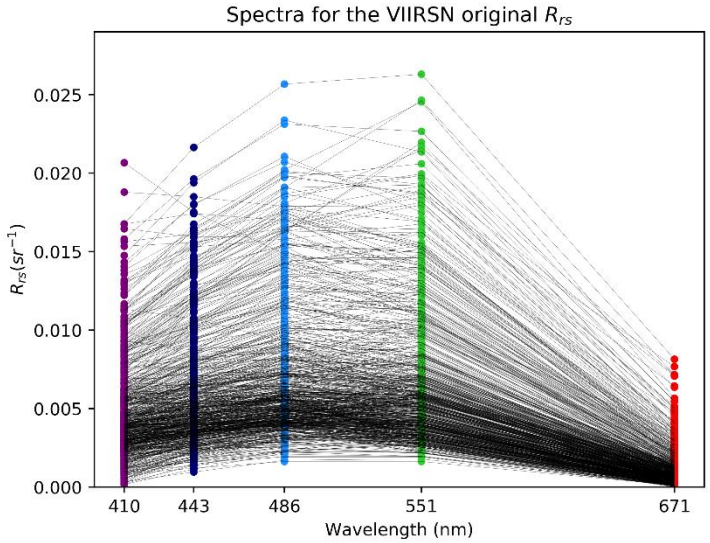

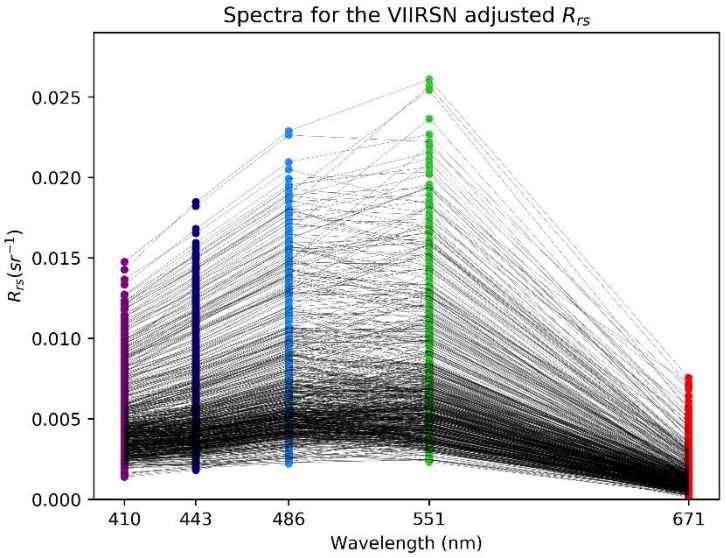

Bracaglia et al., 2019; D'Alimonte et al., 2008; Melin et al. 2011; Zibordi et al., 2006; Zibordi et al.,2009

Multi-linear regression (MLR) adjustment

Different adjustment coefficients for different sensors.
TRAINING DATASET: coefficient calculation.
VALIDATION DATASET: match-up analyses.

$$\Delta R_{rs}(\lambda) = R_{rs}^{is}(\lambda) - R_{rs}^{or}(\lambda)$$

Estimation of the coefficients

$$< \Delta R_{rs}(\lambda) > = a_0^{sat} + \sum_{i=1}^{5} a_i^{sat} R_{rs}^{or}(\lambda_i) + a_6^{sat}\theta_v + a_7^{sat}\theta_s + a_8^{sat}\varphi$$

$$R_{rs}^{adj}(\lambda) = R_{rs}^{or}(\lambda) + < \Delta R_{rs}(\lambda) >$$

Anomalous spectral shape correction.

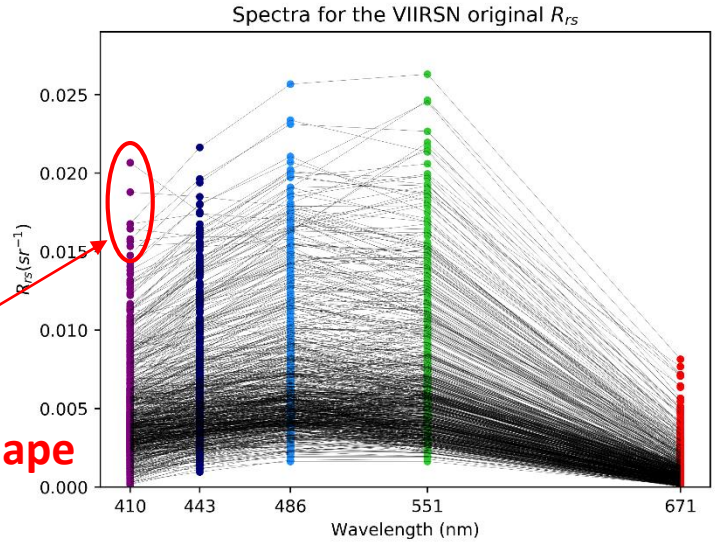

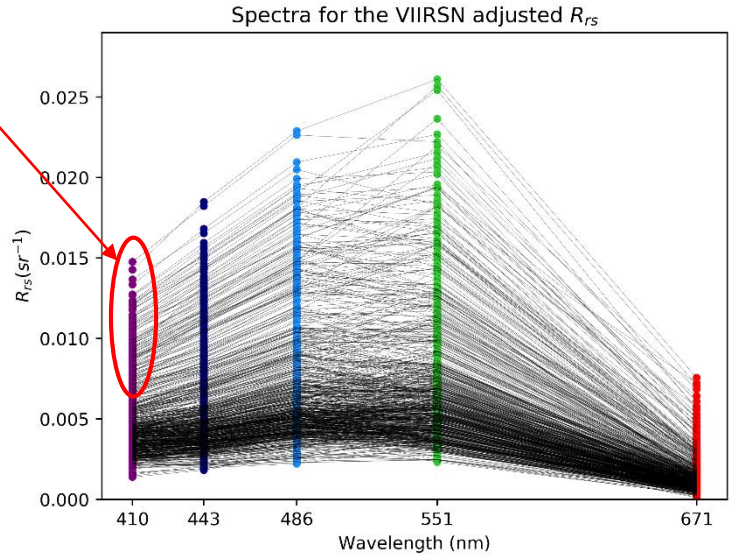

R_{rs}^{or}=original satellite R_{rs}
R_{rs}^{ad}=adjusted satellite R_{rs}
R_{rs}^{is}=in situ R_{rs}

θ_v= sensor zenith angle.
θ_s= solar zenith angle.
ϕ= relative azimuth angle.

Bracaglia et al., 2019; D'Alimonte et al., 2008; Melin et al. 2011; Zibordi et al., 2006; Zibordi et al.,2009

VIIRSN match-up analysis

Training dataset (coefficient calculation): 02/01/2012 - 31/08/2015

Validation dataset (match-up analysis): 01/09/2015 - 28/02/2019

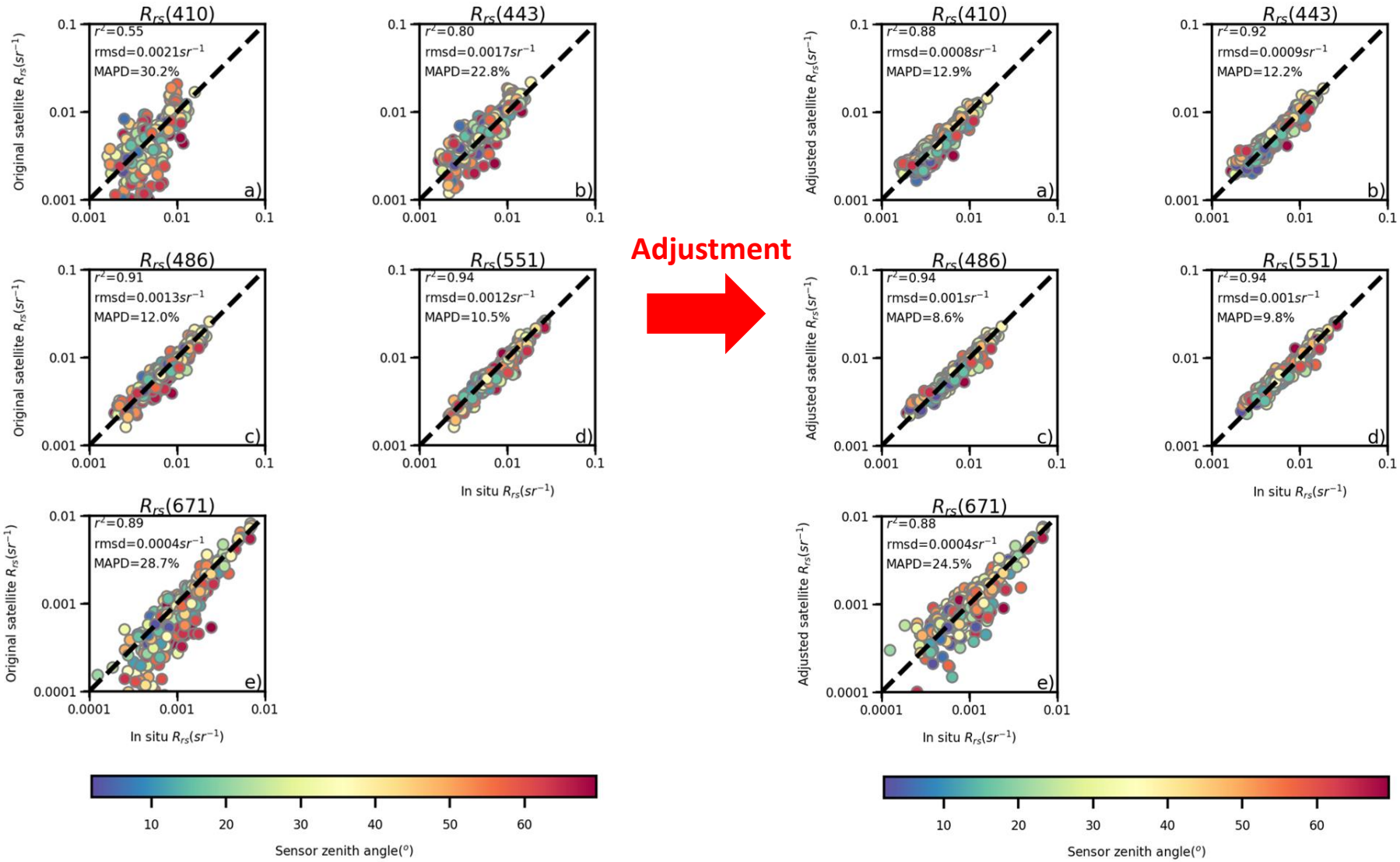

Bracaglia et al., 2019

HSZ flag and sensor zenith angle (θ_v) dependence

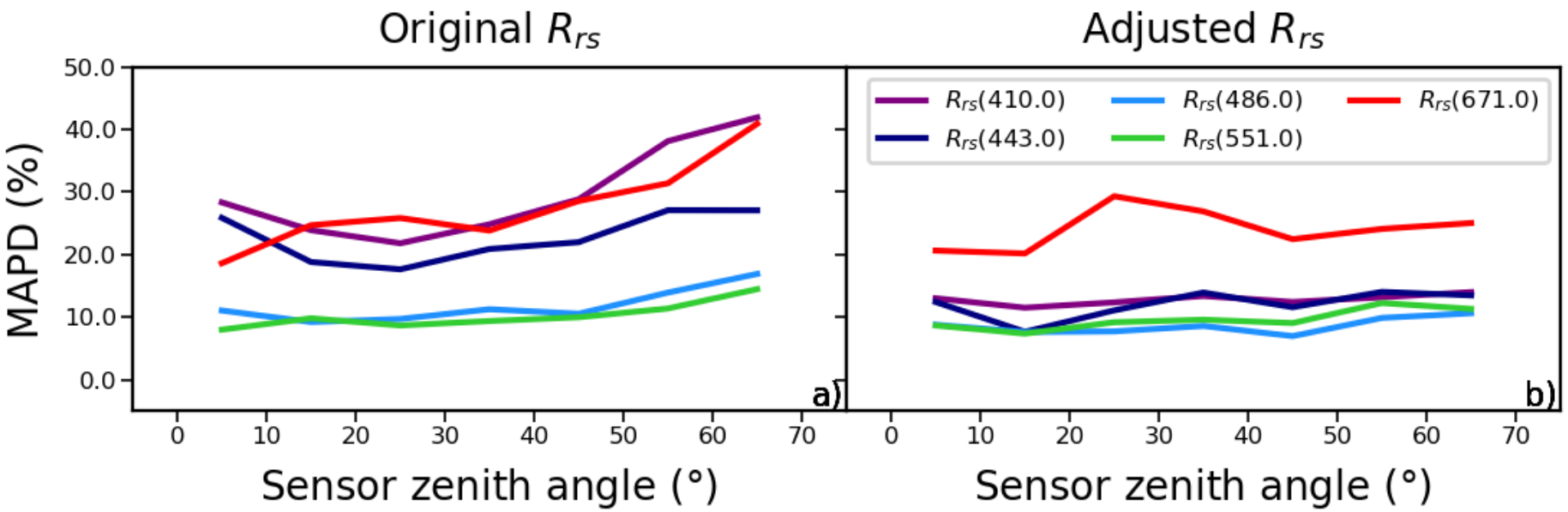

- No application of the High Sensor Zenith flag (HSZ, θ_v>60°).
- Large number of images masked by this flag.
- Calculation of MAPD for different range of θ_v.
- For the original R_{rs} larger uncertainty for MAPD>50°.

Adjustment

- Reduced θ_v dependence.
- Data with θ_v>50° same order of MAPD of those at θ_v<50°.
- Increase of the VGOCS temporal coverage.
- **Up to 3 additional images available during the same day.**

Barnes & Hu, 2016; Bracaglia et al., 2019

Flag and spatial coverage: SL and ANNOT_*

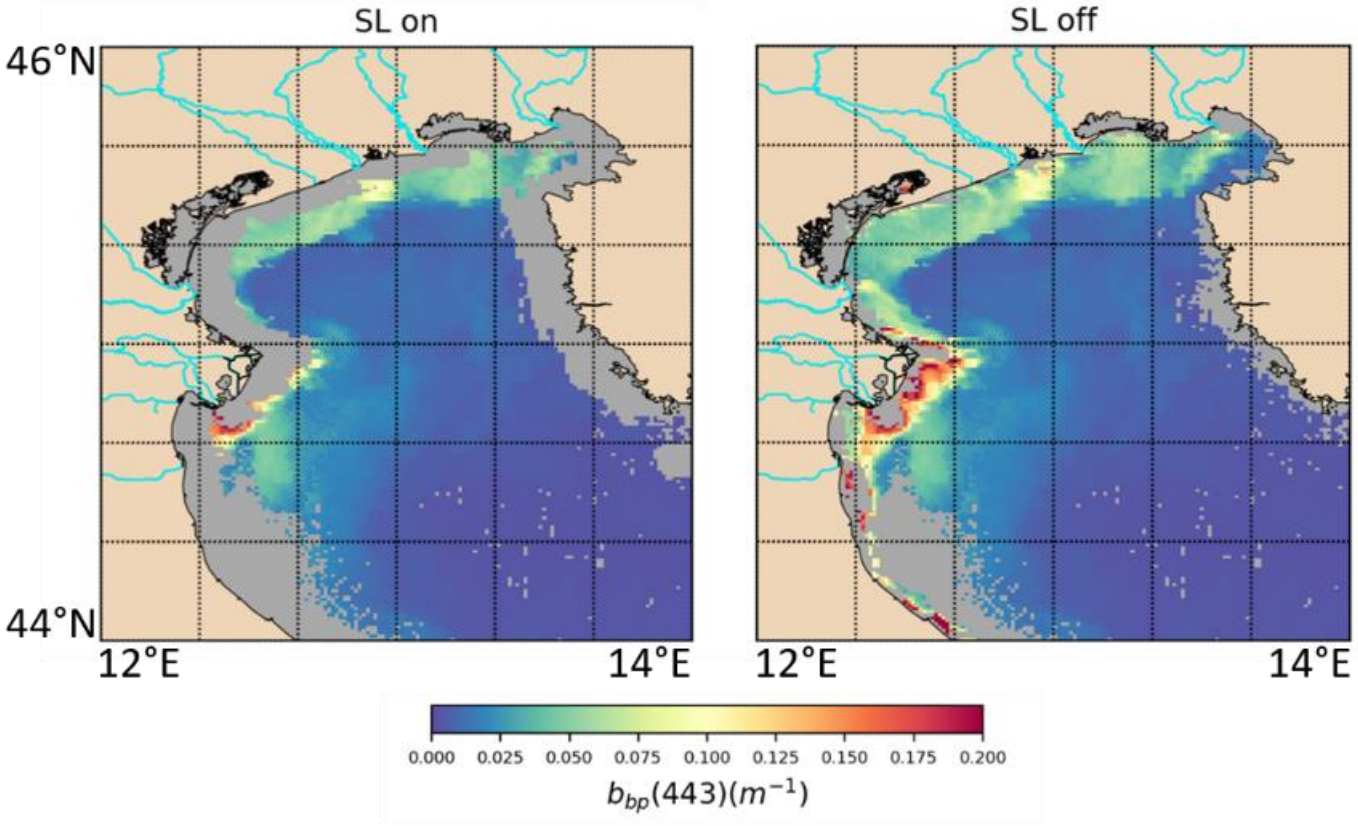

VIIRSN 21/03/2013
12:48 UTC

- Similar effect on spatial coverage with **large number of masked coastal pixels**.
- ANNOT_* data in **good agreement** with the in situ spectra in coastal areas (Zibordi et al.,2018).
- SL uncertainty **strongly reduced by the adjustment.**
- **Notable increase of VGOCS spatial coverage.**
- **SL: 42.4%** additional coastal pixels for NASA sensors.
- **ANNOT_*: 61.6%** additional coastal pixels for OLCI.

Barnes et al., 2019; Bracaglia et al., 2019; Kaufman, 1984; Sterckx et al.,2011; Van Mol and Ruddick, 2005; Zibordi et al., 2018

Inter-sensor differences

- Virtual buoys (red dots and red star).
- Hypothesis:
  - $\Delta R_{rs} \approx 0 sr^{-1}$ for $\Delta t < 20min$.
  - ΔR_{rs} between couple images acquired with $\Delta R_{rs} < 20mins$ are mostly due to artefact .

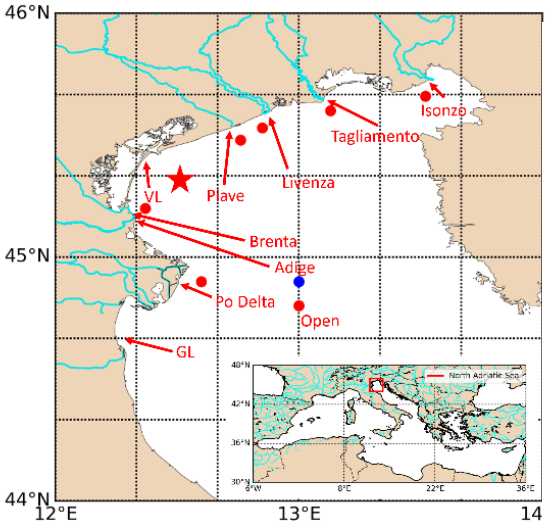

After the adjustment MAPD is reduced spectrally at each virtual buoy.

Reduction of the inter-sensor differences.

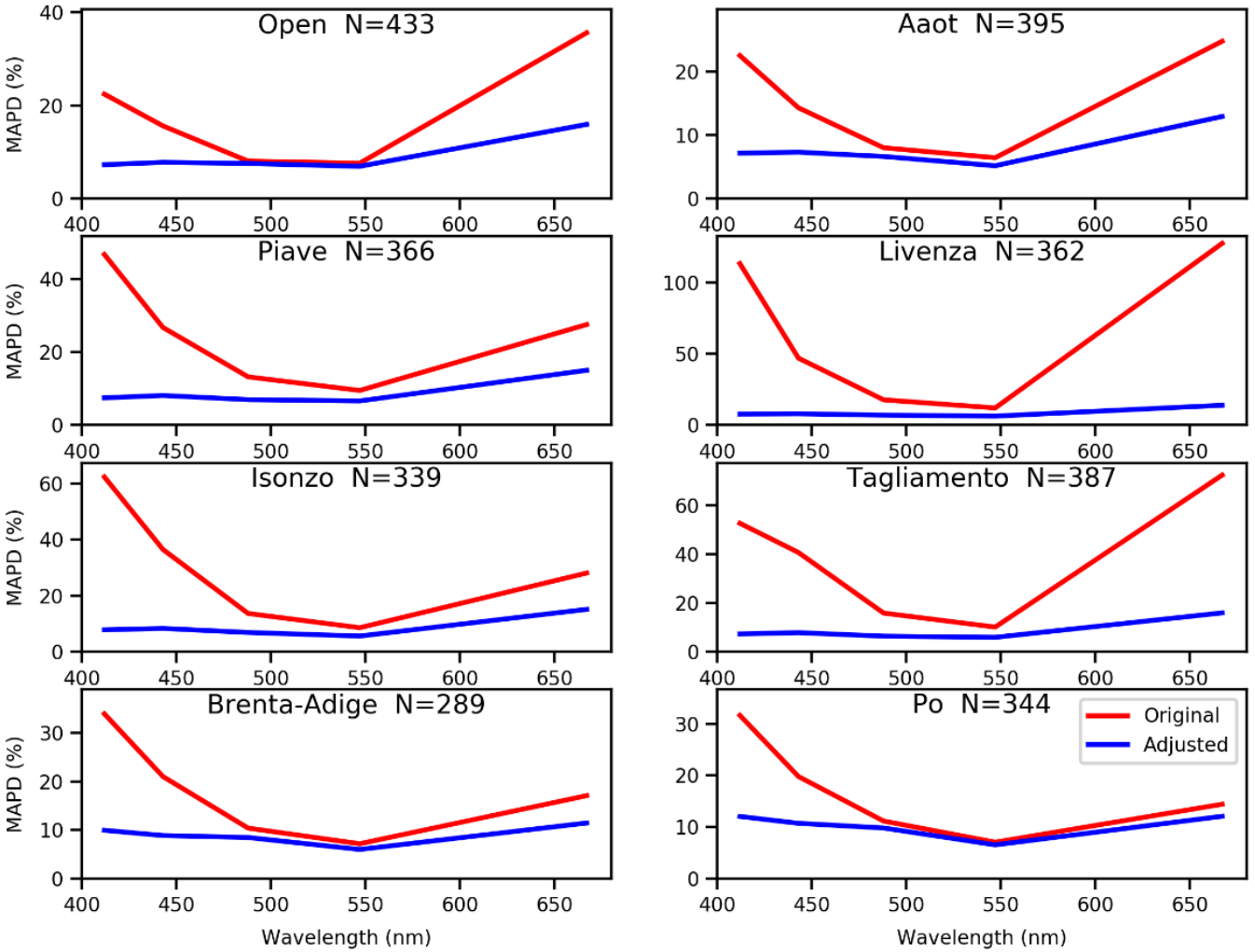

21st and 22nd of March 2013 case study

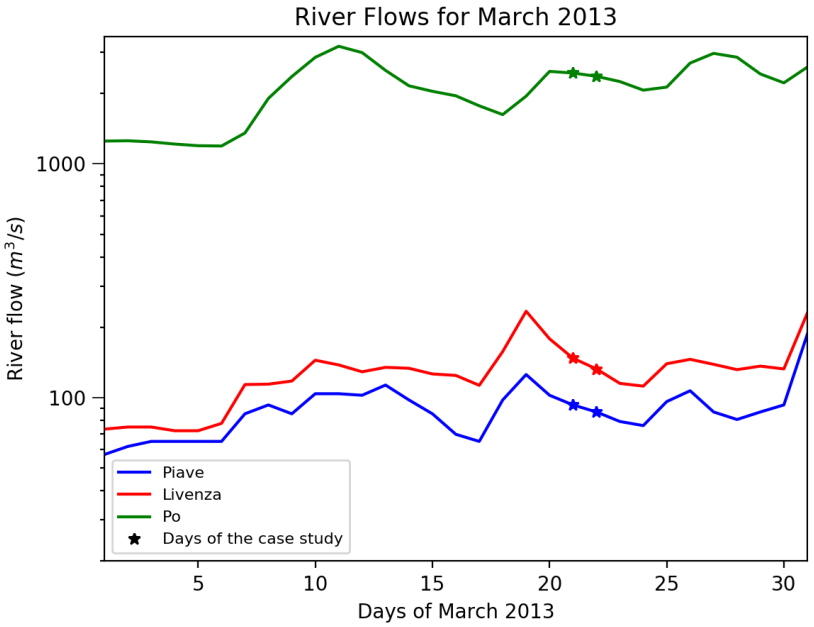

- Analysis of the variability of the particulate backscattering at 443 nm ($b_{bp}(443)$) in the northern part of the basin, using first the CMEMS and then the VGOCS images.
- **High river discharges** for Livenza e Piave during 19th of March; strong reduction in the following days (ARPA data).
- **Strong** $b_{bp}(443)$ reduction between 21st and 22nd of March.
- How and when did this reduction take place during the 24 hours?
- **No information close to the shore (stray-light flag).**

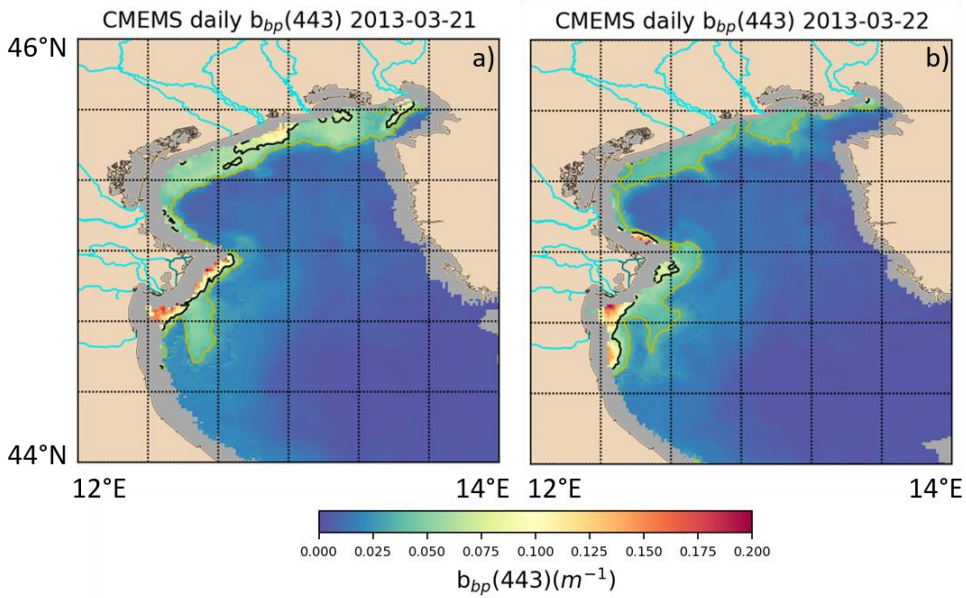

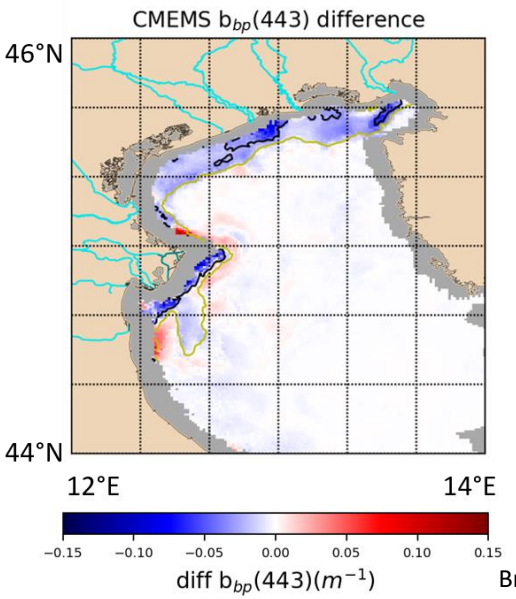

Bracaglia et al., 2019

VGCOS images: 21st of March

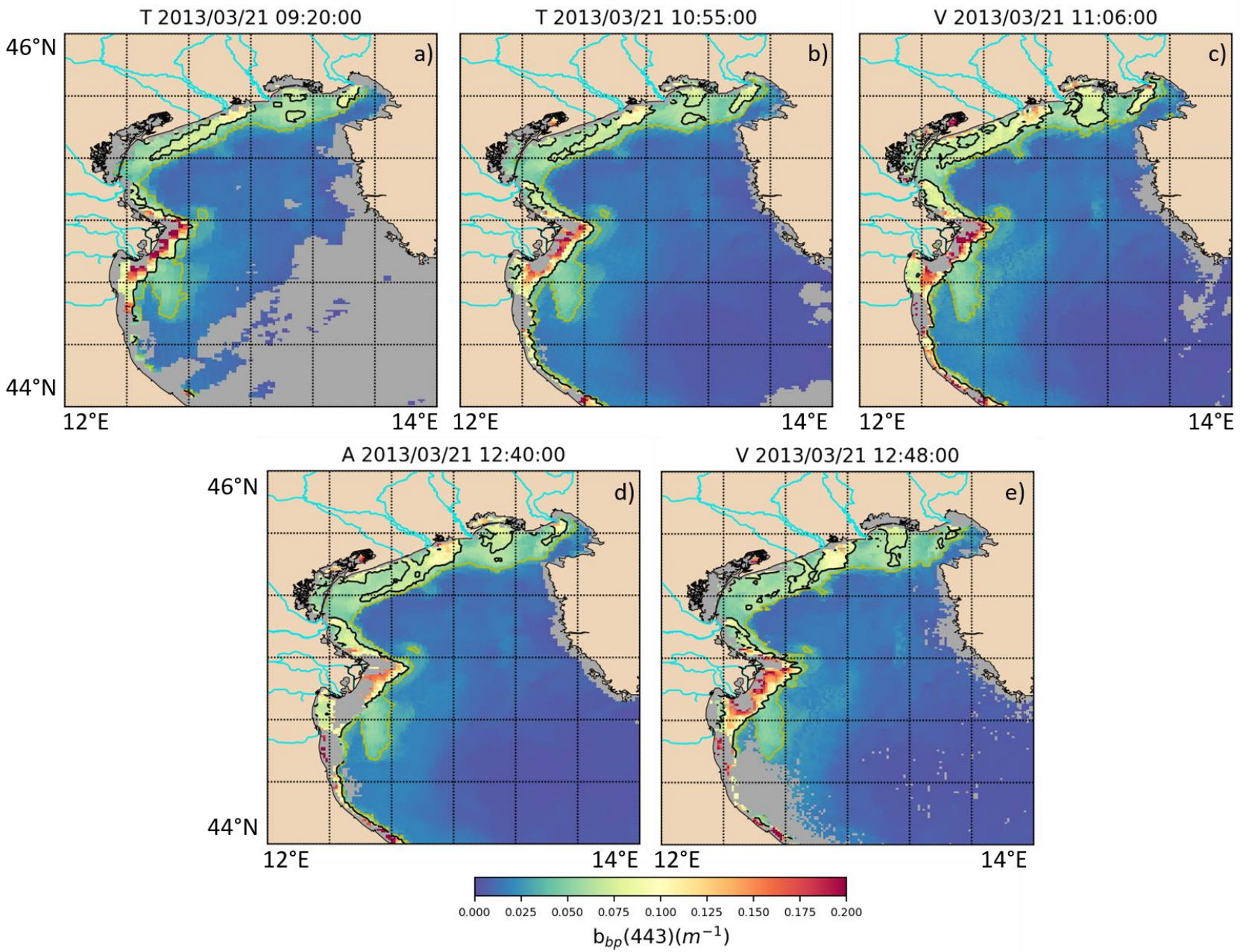

VGCOS images: 21st of March

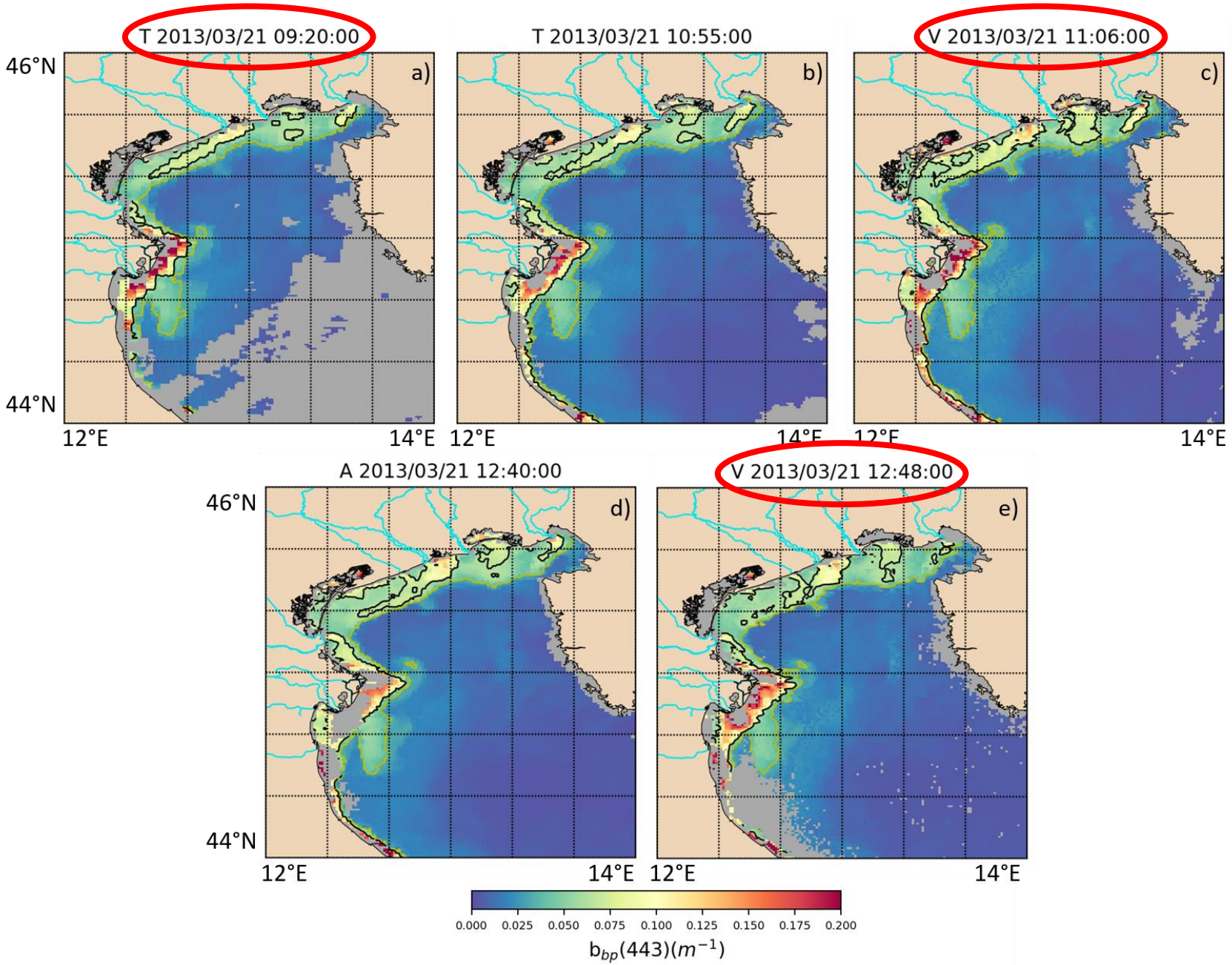

VGOCS: 21st of March variability

Evolution between 09:20 and 11:06 UTC

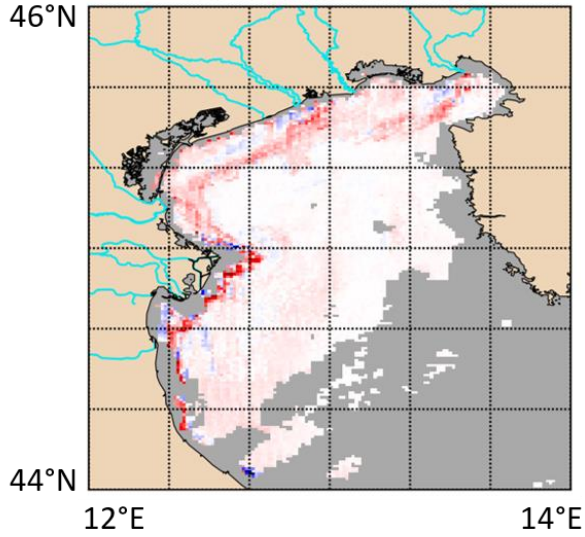

Evolution between 11:06 and 12:48 UTC

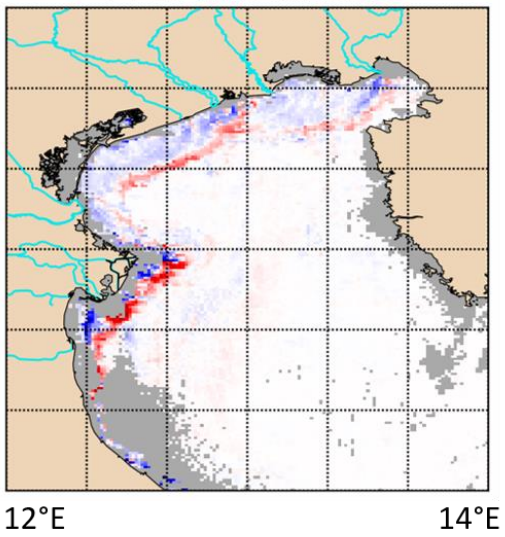

- Increase of $b_{bp}(443)$ between 09:20 e 11:06 UTC due to the particulate matter carried by the river.
- After 11:06 strong reduction close to the river mouths.
- In 3 hours and half: reduction close to the river mouths, increase far from the shore for southward advection of the particulate matter.

Evolution between 09:20 and 12:48 UTC

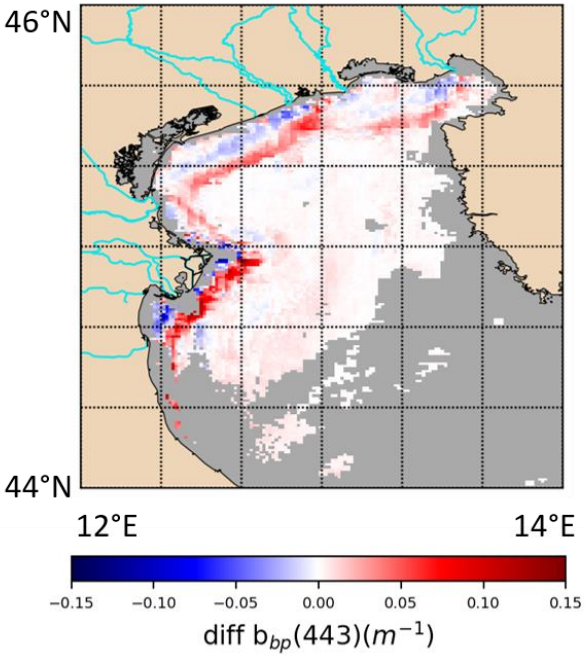

Black isolines:
$b_{bp}(443)=0.065m^{-1}$

Yellow isolines:
$b_{bp}(443)=0.035m^{-1}$

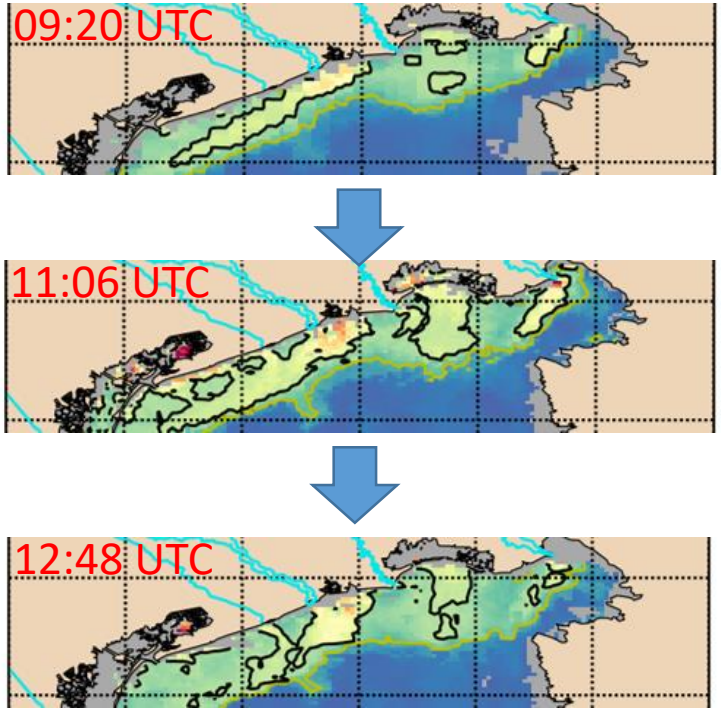

VGCOS: inter-daily and 22nd of March variability.

Evolution between 12:48 UTC of the 21° of March and 10:00 UTC of 22° of March

Evolution between 10:00 and 13:06 UTC of 22° of March

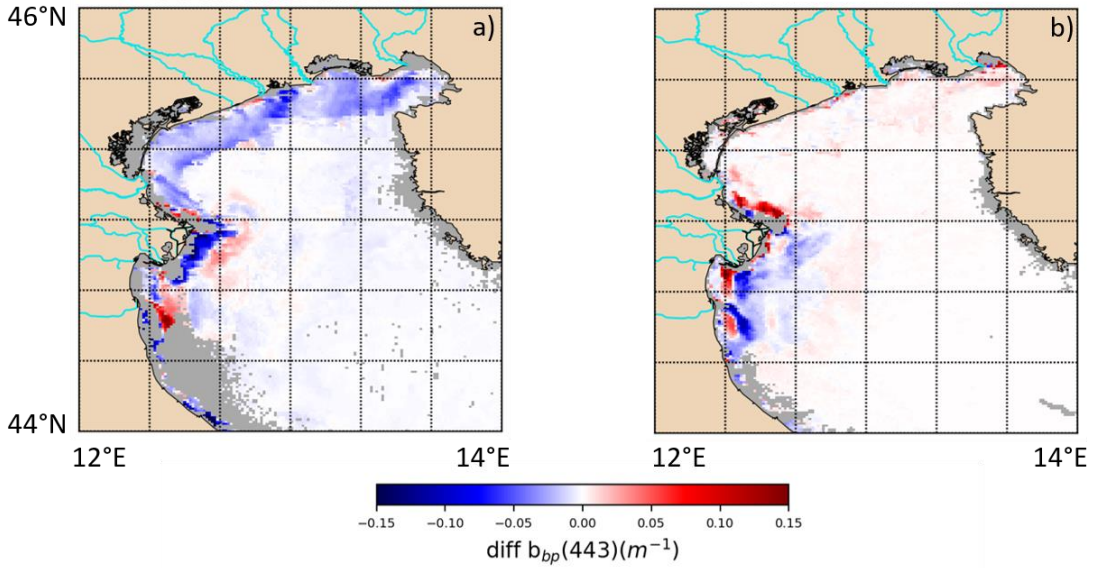

- Strong reduction between the two days, as for the CMEMS product.
- Multiple images allowed to capture most of the optical variability during the two days.
- Information about the dynamics and the dispersion of the particulate matter into the basin, not feasible with a daily product.
- Information close to the river mouths due to unmasking for SL.

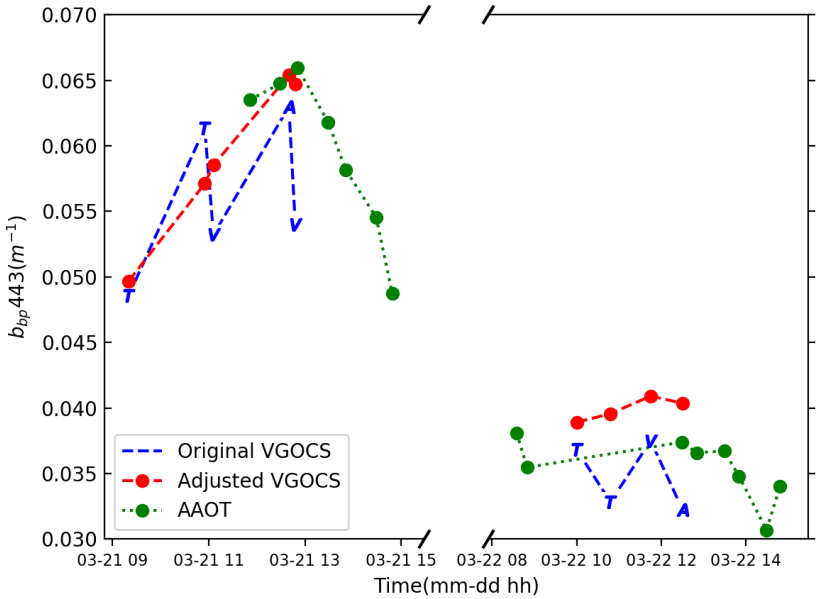

- Better agreement for the adjusted $b_{bp}(443)$ with the one retrieved from the in situ data.
- Lower $b_{bp}(443)$ difference for the adjusted product for observations acquired in temporal proximity.

VGCOS: inter-daily and 22nd of March variability.

Evolution between 12:48 UTC of the 21° of March and 10:00 UTC of 22° of March

Evolution between 10:00 and 13:06 UTC of 22° of March

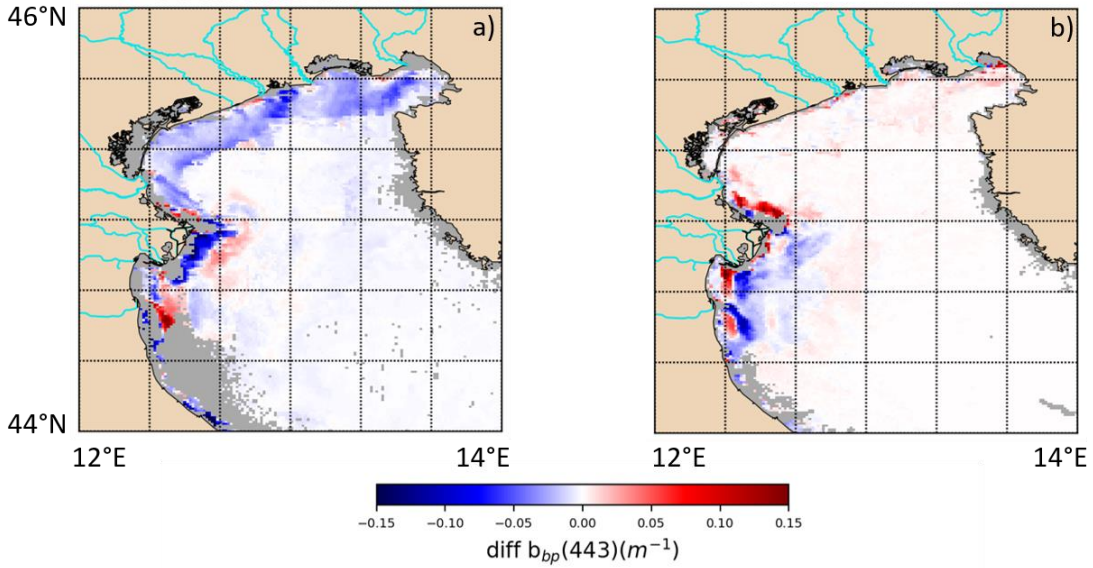

- Strong reduction between the two days, as for the CMEMS product.
- Multiple images allowed to capture most of the optical variability during the two days.
- Information about the dynamics and the dispersion of the particulate matter into the basin, not feasible with a daily product.
- Information close to the river mouths due to unmasking for SL.

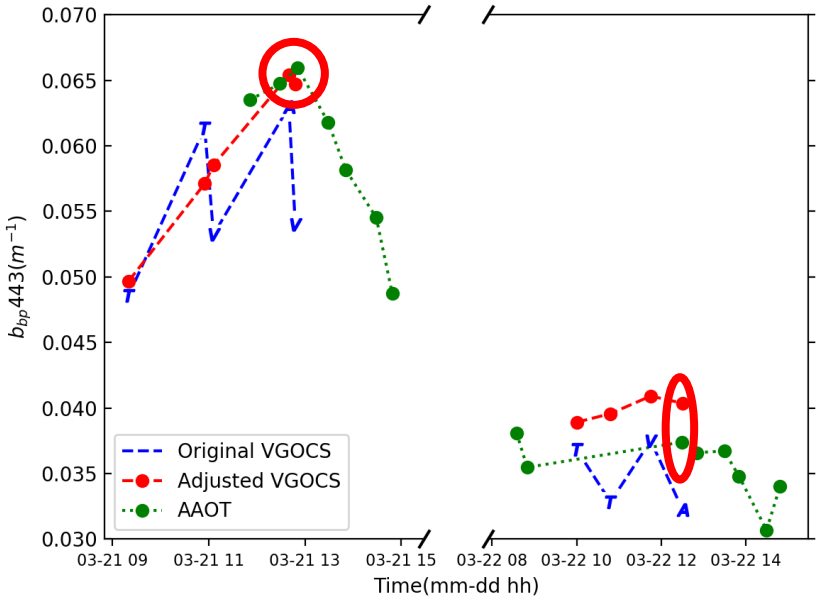

- Better agreement for the adjusted $b_{bp}(443)$ with the one retrieved from the in situ data.
- Lower $b_{bp}(443)$ difference for the adjusted product for observations acquired in temporal proximity.

VGCOS: inter-daily and 22nd of March variability.

Evolution between 12:48 UTC of the 21° of March and 10:00 UTC of 22° of March

Evolution between 10:00 and 13:06 UTC of 22° of March

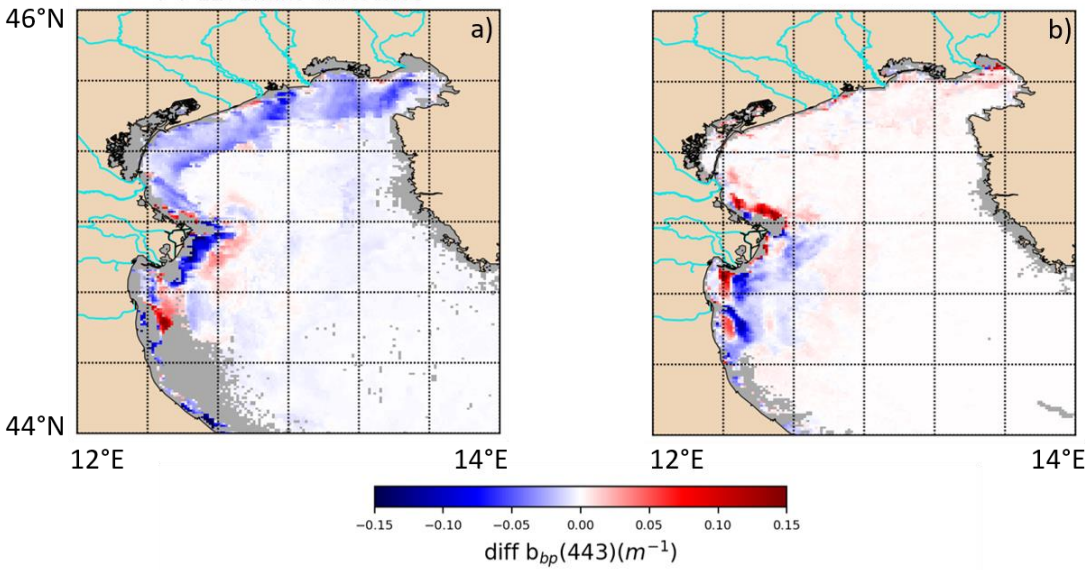

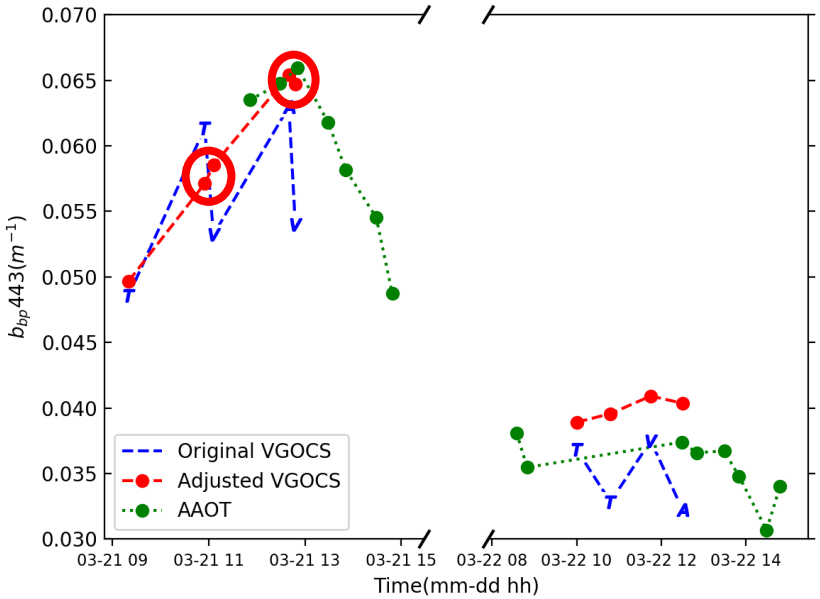

- Strong reduction between the two days, as for the CMEMS product.
- Multiple images allowed to capture most of the optical variability during the two days.
- Information about the dynamics and the dispersion of the particulate matter into the basin, not feasible with a daily product.
- Information close to the river mouths due to unmasking for SL.

- Better agreement for the adjusted $b_{bp}(443)$ with the one retrieved from the in situ data.
- Lower $b_{bp}(443)$ difference for the adjusted product for observations acquired in temporal proximity.

Conclusions

- Adjustment improved the agreement with the in situ data, reduced the inter-sensor differences and allowed to use data generally masked in the standard processing chains:
  - No HSZ flag make available up to 3 additional images of the basin.
  - No SL flag for NASA (+ 42.4%) and no ANNOT_* flag for OLCI (+61.6%) allow to have information on coastal pixels.
- Need of an OC geostationary sensor over the european seas, partially compensated by our datasets.
- VGOCS analysis ready dataset allows to have at disposal more images of the basin during the same day, approaching a geostationary sensor temporal resolution.

Conclusions and future perspectives

- VGOCS analysis ready dataset allows the users to:
  - Use OC data without a pre-processing, in order to have a quick access to field such R_{rs} spectra and various IOPs.
  - Calculate IOPs and component concentration using different algorithms, with the adjusted R_{rs} spectra as input.
  - Perform analysis exploiting products usually not provided in standard L3 files, such flags and viewing geometry parameters.
- Next steps:
  - Analyse the tidal effect on sediment transport and river plume dynamics.
  - Extend the approach in other coastal areas, where at least one automatic radiometric station representative of the entire basin optical variability is present (as in the Western Black Sea, Baltic Sea, Northern Sea).

Thanks for your attention.

This study was supported by PhD Fellowship at Università degli Studi di Napoli Parthenope, the Ocean Colour Thematic Assembly Centre of the Copernicus Marine Environment and Monitoring Service (grant number: 77-CMEMS-TAC-OC), the EU H2020 CoastObs Project (GA no 776348)